# The "$\eta$-sweet-spot" ($\eta_{max}$) in liquid-assisted mechanochemistry: the liquid additive as a catalyst and an inhibitor in resonant acoustic mixing (RAM)

Lori Gonnet,[a] Tristan H. Borchers,[a] Cameron B. Lennox,[a] Jogirdas Vainauskas,[a] Yong Teoh, [a] Hatem M. Titi,[a] Christopher J. Barrett,[a] Stefan G. Koenig,*[b] Karthik Nagapudi,*[b] and Tomislav Friščić*[a]

[a] *Department of Chemistry, McGill University. 801 Sherbrooke St. West, Montreal, QC, H3H 0B8, Canada*
[b] *Small molecule Pharmaceutical Sciences, Genentech Inc., One DNA Way, South San Francisco, CA 94080, USA.*

## Table of Contents

## 1. Materials and methods

The $^{1}H$ and $^{13}C$ nuclear magnetic resonance spectroscopy (NMR) analyses were performed using a Bruker 800 MHz nuclear magnetic resonance spectrometer. The NMR chemical shifts are reported relative to $d_6$-DMSO (δ 2.50) and the data is presented as chemical shifts and integration. The molecular weights of the purified products were obtained using high-resolution mass spectroscopy (HRMS). Powder X-ray diffraction (PXRD) analysis was performed over the $2\theta$-range from 4° to 40°, using a Bruker D2 PHASER X-ray diffractometer equipped with a Cu$K_\alpha$ (λ = 1.5406 Å) source, LinxEye detector, and a nickel filter. Single crystal X-Ray Diffraction (SCXRD) data was measured on a Bruker D8 Venture diffractometer equipped with a Photon 200 detector, and an *IμS* microfocus X-ray source (Bruker AXS, CuKα source). All measurements were carried out at 298(2) K on crystals coated with a thin layer of amorphous oil. Structure solution was carried out using the SHELXTL package from Bruker.[1] The parameters were refined for all data by full-matrix-least-squares on $F^2$ using SHELXL[2] within the OLEX2[3] and/or SHELXLE8[4] environment. All the non-hydrogen atoms were refined with anisotropic thermal parameters. All other hydrogen atoms were placed in calculated positions and allowed to ride on the carrier atoms. All hydrogen atom thermal parameters were constrained to ride on the carrier atom.

## 2. General procedure for the RAM synthesis of compounds 1-10

In a typical experiment, the sulfonamide (0.5 mmol, 1 eq), carbodiimide (0.5 mmol, 1 eq) and CuCl (5 mol%) were added to a 2.5 mL polypropylene vial. 2-Butanone (η = 0.0251 μL/mg) was added to the vial and the mixture mixed using the LabRAM II instrument between 15 minutes and 2 hours, at an acceleration between 30 and 90 g. The conversion was evaluated by $^{1}H$ NMR analysis of a solution obtained by dissolving the entire crude reaction mixture in d6-DMSO. The sulfonyl-ureas 1−10 were isolated by mixing of the reaction mixture for additional 10 min at 60 g in the presence of a saturated aqueous solution of EDTA (1 mL), followed by filtration. Recrystallization of the product from hot ethanol removed remaining brown-colored residues, and the resulting white to yellow solid was then filtered and dried in air.

## 3. Reaction conversion data for studies illustrated in the manuscript

**Table S1.** Conversion of *p*-toluenesulfonamide and DCC to the sulfonylguanidine **1**, following RAM in the presence of 5 mol% CuCl and different amounts (given as $\eta$, in μL/mg) of EtOAc, MeOBz, acetone, 2-butanone, DMF and $MeNO_2$ as the liquid additive. All reactions were performed on 0.5 mmol scale and the deviations from the mean value were established by performing each reaction in triplicate. No reaction was observed at $\eta$ = 0 μL/mg.

| $\eta$ (μL/mg) | EtOAc | MeOBz | acetone | 2-butanone | DMF | $MeNO_2$ |
|---|---|---|---|---|---|---|
| 0.25 | 21 ± 3 | 23 ± 3 | 10 ± 2 | 41 ± 3 | 92 ± 2 | 21 ± 2 |
| 0.50 | 4 ± 1 | 13 ± 2 | 5 ± 1 | 17 ± 2 | 93 ± 1 | 12 ± 2 |
| 0.75 | 4 ± 1 | 8 ± 1 | 3 ± 1 | 15 ± 2 | 91 ± 2 | 11 ± 2 |
| 1.0 | 3 ± 1 | 7 ± 1 | 3 ± 1 | 10 ± 1 | 90 ± 2 | 10 ± 1 |

**Table S2.** Conversion of different sulfonamide reactants to corresponding sulfonylguanidines **1-5** upon RAM in the presence of one equivalent DCC, 5 mol% CuCl catalyst and different amounts of 2-butanone liquid additive, in the $\eta$ range 0 to 1 μL/mg. All reactions were performed on 0.5 mmol scale and the deviations from the mean value were established by performing each reaction in triplicate.

| $\eta$ (μL/mg) | **1** | **2** | **3** | **4** | **5** |
|---|---|---|---|---|---|
| 0 | 0 ± 0 | 0 ± 0 | 0 ± 0 | 0 ± 0 | 0 ± 0 |
| 0.01 | 9 ± 1 | 15 ± 2 | 11 ± 2 | 12 ± 2 | 9 ± 2 |
| 0.025 | 70 ± 3 | 64 ± 3 | 61 ± 3 | 66 ± 3 | 27 ± 3 |
| 0.05 | 66 ± 2 | 59 ± 2 | 50 ± 2 | 64 ± 2 | 25 ± 2 |
| 0.07 | 55 ± 3 | 53 ± 3 | 43 ± 3 | 50 ± 3 | 22 ± 2 |
| 0.10 | 47 ± 4 | 48 ± 2 | 35 ± 3 | 39 ± 3 | 20 ± 3 |
| 0.17 | 45 ± 3 | 44 ± 3 | 25 ± 2 | 34 ± 1 | 19 ± 2 |
| 0.25 | 41 ± 2 | 29 ± 3 | 22 ± 3 | 26 ± 4 | 18 ± 2 |
| 0.37 | 23 ± 2 | 18 ± 2 | 17 ± 1 | 24 ± 2 | 14 ± 1 |
| 0.50 | 17 ± 2 | 15 ± 2 | 14 ± 2 | 17 ± 2 | 12 ± 2 |
| 0.75 | 15 ± 2 | 11 ± 2 | 6 ± 1 | 12 ± 2 | 10 ± 2 |
| 1.00 | 10 ± 1 | 7 ± 2 | 5 ± 1 | 10 ± 2 | 8 ± 1 |

**Table S3.** Conversion of different sulfonamide reactants to corresponding sulfonylguanidines **6-10** upon RAM by reaction with DIC, in the presence of 5 mol% CuCl catalyst and 2-butanone liquid additive in the $\eta$ range 0 to 0.75 μL/mg. All reactions were performed on 0.5 mmol scale and the deviations from the mean value were established by performing each reaction in triplicate.

| $\eta$ (μL/mg) | **6** | **7** | **8** | **9** | **10** |
|---|---|---|---|---|---|
| 0 | 60 ± 2 | 60 ± 2 | 45 ± 2 | 64 ± 2 | 26 ± 3 |
| 0.07 | 75 ± 3 | 66 ± 3 | 55 ± 3 | 66 ± 3 | 30 ± 2 |
| 0.10 | 90 ± 2 | 81 ± 2 | 65 ± 3 | 70 ± 2 | 35 ± 3 |
| 0.25 | 72 ± 2 | 49 ± 4 | 44 ± 2 | 53 ± 2 | 33 ± 2 |
| 0.50 | 47 ± 3 | 34 ± 3 | 25 ± 2 | 29 ± 3 | 17 ± 2 |
| 0.75 | 22 ± 2 | 18 ± 2 | 12 ± 2 | 18 ± 2 | 7 ± 1 |

## 4. Crystallographic data for compound 1

**Table S4**. Crystallographic data for compound **1** polymorphs Form I and II.

| | Form I (CSD code: KOPPOW) | Form II |
|---|---|---|
| Molecular formula | $C_{20}H_{31}N_3O_2$ | $C_{20}H_{31}N_3O_2$ |
| $M_r$ | 377.54 | 377.54 |
| Crystal system | Triclinic | Trigonal |
| Crystal colour | Colorless | Colorless |
| Space group | P-1 | R-3 |
| Temperature (K) | 293 | 298 |
| Unit cell dimensions (Å,°) | | |
| *a* | 12.075(3) | 23.2800(4) |
| *b* | 12.703(3) | 23.2800(4) |
| *c* | 15.167(4) | 19.9119(4) |
| $\alpha$ | 92.220(3) | 90 |
| $\beta$ | 109.140(3) | 90 |
| $\gamma$ | 106.008(3) | 120 |
| Volume (Å$^3$) | 2091.2(9) | 9345.6(4) |
| Z | 4 | 18 |
| $\rho_{calc}$ (g cm$^{-3}$) | 1.199 | 1.207 |
| $\mu$ (mm$^{-1}$) | 0.173 | 1.525 |
| F(000) | 816 | 3672.0 |
| Refl. Collected/independent | 19658/7231 | 49799/3921 |
| No. observed refl. [I>2σ(*I*)]* | 5001 | 2775 |
| No. restraints/No. parameters | 0/475 | 0/236 |
| *R/wR* [all data] | 0.0816/0.1601 | 0.0783/0.1595 |
| Goodness-of-fit on $F^2$ | 1.049 | 1.137 |

*$R = \sum||Fo|-|Fc||/\sum Fo, w = 1/[\sigma^2(Fo^2)+(g_1P)^2+ g^2P]$ where $P = (Fo^2+2Fc^2)/3$, $S = \Sigma[w(Fo^2 – Fc^2)^2/(N_{obs} – N_{param})]^{1/2}$.

## 5. DSC analysis of 1, polymorph Form I and II

DSC analysis was performed to determine the melting point of pure compound **1** Form II and II. A DSC 2500 equipment (TA instrument) was used. All analyses were performed at 10 °C/min from 25 to 300 °C.

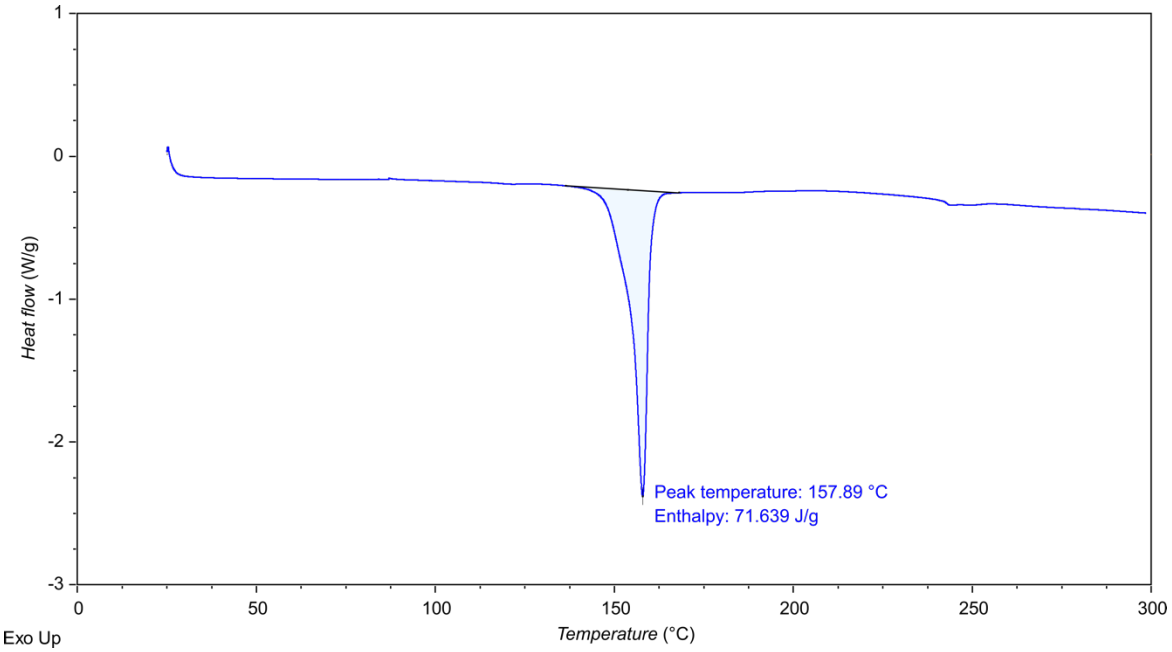


**Figure S1.** DSC thermograms for isolated compound **1**, polymorph Form I.

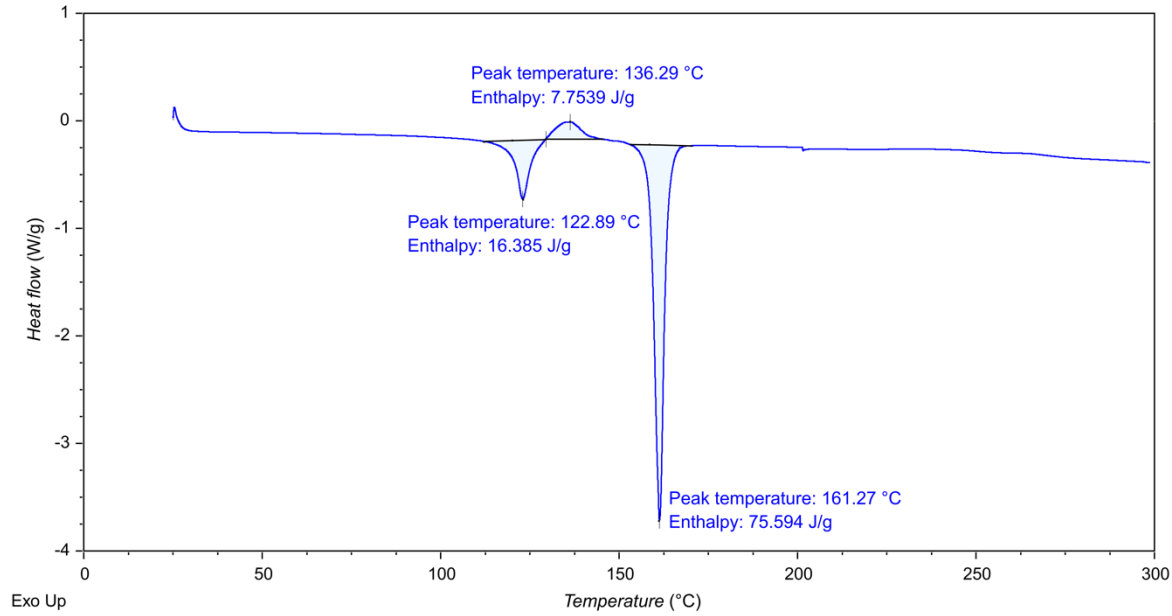


**Figure S2.** DSC thermograms for isolated compound **1**, polymorph Form II.

## 6. Summary of $^{1}H$ and $^{13}C$ NMR and HR-MS Data

***N*-(bis(cyclohexylamino)methylene)-4-methylbenzenesulfonamide 1**

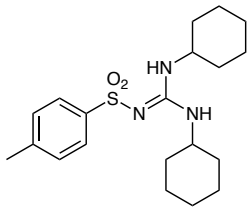

$^{1}H$ NMR (800 MHz, DMSO) δ 7.59 (d, *J* = 8.0 Hz, 2H), 7.30 (d, *J* = 8.0 Hz, 2H), 6.83 (d, *J* = 126.1 Hz, 2H), 3.53 (s, 2H), 2.35 (s, 3H), 1.73 – 1.52 (m, 10H), 1.28 – 1.04 (m, 10H). $^{13}C$ NMR (800 MHz, DMSO) δ 153.83, 142.06, 141.59, 129.55, 125.89, 40.46, 32.68, 25.43, 21.34. HRMS ESI (+): Calculated for $C_{20}H_{32}O_2N_3S$ $[M+H]^+$: 378.22097; measured: 378.22221.

***N*-(bis(cyclohexylamino)methylene)-2-methylbenzenesulfonamide 2**

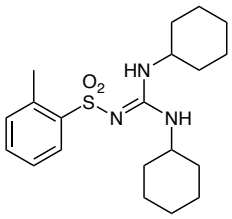

$^{1}H$ NMR (800 MHz, DMSO) δ 7.79 (d, *J* = 7.8 Hz, 1H), 7.42 (t, *J* = 7.5 Hz, 1H), 7.33 – 7.29 (m, 2H), 6.86 (s, 2H), 3.56 (s, 2H), 2.59 (s, 3H), 1.72 – 1.46 (m, 10H), 1.20 – 1.04 (m, 10H). $^{13}C$ NMR (800 MHz, DMSO) δ 153.61, 142.59, 136.55, 132.45, 131.76, 127.16, 125.93, 50.46, 32.76, 25.41, 24.17, 20.08. HRMS ESI (+): Calculated for $C_{20}H_{32}O_2N_3S$ $[M+H]^+$: 378.22097; measured: 378.21986.

***N*-(bis(cyclohexylamino)methylene)benzenesulfonamide 3**

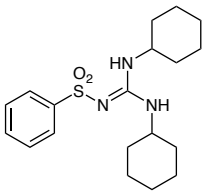

$^{1}H$ NMR (800 MHz, DMSO) δ 7.71 – 7.70 (m, 2H), 7.54 – 7.49 (m, 3H), 6.87 (s, 2H), 3.56 (s, 2H), 1.73 – 1.50 (m, 10H), 1.27 – 0.95 (m, 10H). $^{13}C$ NMR (800 MHz, DMSO) δ 153.88, 144.77, 131.66, 129.16, 125.84, 40.46, 33.82, 32.72, 25.79, 25.43, 25.12. HRMS ESI (+): Calculated for $C_{19}H_{30}O_2N_3S$ $[M+H]^+$: 364.20532; measured: 364.20419.

***N*-(bis(cyclohexylamino)methylene)-4-chlorobenzenesulfonamide 4**

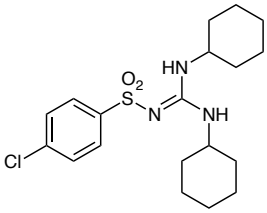

$^{1}H$ NMR (800 MHz, DMSO) δ 7.72 – 7.70 (m, 2H), 7.60 – 7.58 (m, 2H), 6.87 (s, 2H), 3.56 (s, 2H), 1.71 – 1.49 (m, 10H), 1.29 – 1.07 (m, 10H). $^{13}C$ NMR (800 MHz, DMSO) δ 153.79, 143.66, 136.35, 129.31, 127.85, 40.46, 32.66, 25.40, 24.66. HRMS ESI (+): Calculated for $C_{19}H_{29}O_2N_3ClS$ $[M+H]^+$: 398.16635; measured: 398.16581.

***N*-(bis(cyclohexylamino)methylene)-4-methoxybenzenesulfonamide 5**

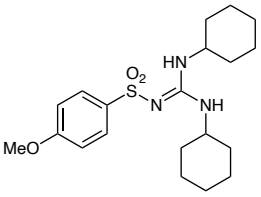

$^{1}H$ NMR (800 MHz, DMSO) δ 7.64 – 7.62 (m, 2H), 7.04 – 7.02 (m, 2H), 6.80 (d, *J* = 138.4 Hz, 2H), 3.80 (s, 3H), 3.56 (s, 2H), 1.69 – 1.49 (m, 10H), 1.28 – 1.04 (m, 10H). $^{13}C$ NMR (800 MHz, DMSO) δ 161.64, 153.79, 136.91, 127.83, 114.23, 55.95, 40.46, 32.74, 25.45 24.08. HRMS ESI (+): Calculated for $C_{20}H_{32}O_3N_3S$ $[M+H]^+$: 394.21589; measured: 394.21557.

***N*-(bis(isopropylamino)methylene)-4-methylbenzenesulfonamide 6**

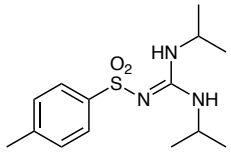

$^1$H NMR (500 MHz, DMSO) δ 7.62 – 7.60 (m, 2H), 7.31 – 7.29 (m, 2H), 6.77 (s, 2H), 3.86 (s, 2H), 2.35 (s, 3H), 1.04 (d, *J* = 6.5 Hz, 12H). $^{13}$C NMR (500 MHz, DMSO) δ 153.95, 142.08, 141.58, 129.53, 125.97, 43.00, 22.84, 21.34. HRMS ESI (+): Calculated for $C_{14}H_{24}O_2N_3S$ $[M+H]^+$: 298.15837; measured: 298.15944.

***N*-(bis(isopropylamino)methylene)-2-methylbenzenesulfonamide 7**

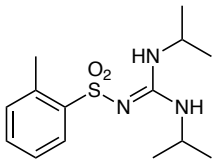

$^1$H NMR (500 MHz, DMSO) δ 7.81 (dd, *J* = 7.8, 1.4 Hz, 1H), 7.42 (td, *J* = 7.4, 1.4 Hz, 1H), 7.34 – 7.29 (m, 2H), 6.74 (d, *J* = 8.2 Hz, 2H), 3.87 (s, 2H), 2.58 (s, 3H), 1.03 (d, *J* = 6.4 Hz, 12H). $^{13}$C NMR (500 MHz, DMSO) δ 153.79, 142.65, 136.54, 132.45, 131.76, 127.28, 125.92, 43.01, 22.85, 20.14. HRMS ESI (+): Calculated for $C_{14}H_{24}O_2N_3S$ $[M+H]^+$: 298.15837; measured: 298.15817.

***N*-(bis(isopropylamino)methylene)benzenesulfonamide 8**

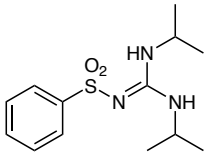

$^1$H NMR (500 MHz, DMSO) δ 7.74 – 7.72 (m, 2H), 7.55 – 7.49 (m, 3H), 6.80 (d, *J* = 8.1 Hz, 2H), 3.86 (s, 2H), 1.03 (d, *J* = 6.4 Hz, 12H). $^{13}$C NMR (500 MHz, DMSO) δ 154.00, 144.80, 131.66, 129.13, 125.91, 43.05, 22.82. HRMS ESI (+): Calculated for $C_{13}H_{22}O_2N_3S$ $[M+H]^+$: 284.14272; measured: 284.14232.

***N*-(bis(isopropylamino)methylene)-4-chlorobenzenesulfonamide 9**

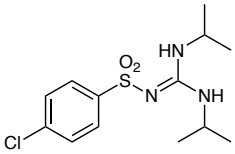

$^1$H NMR (500 MHz, DMSO) δ 7.75 – 7.72 (m, 2H), 7.60 – 7.57 (m, 2H), 6.82 (d, *J* = 8.0 Hz, 2H), 3.86 (s, 2H), 1.04 (d, *J* = 6.5 Hz, 12H). $^{13}$C NMR (500 MHz, DMSO) δ 153.90, 143.69, 136.35, 129.27, 127.93, 43.12, 22.80. HRMS ESI (+): Calculated for $C_{13}H_{21}O_2N_3ClS$ $[M+H]^+$: 318.10375; measured: 318.10331.

***N*-(bis(isopropylamino)methylene)-4-methoxybenzenesulfonamide 10**

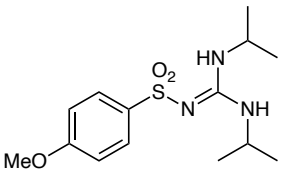

$^1$H NMR (500 MHz, DMSO) δ 7.67 – 7.64 (m, 2H), 7.04 – 7.01 (m, 2H), 6.78 – 6.73 (m, 2H), 3.83 (s, 2H), 3.80 (s, 3H), 1.04 (d, *J* = 6.4 Hz, 12H). $^{13}$C NMR (500 MHz, DMSO) δ 161.64, 153.91, 136.94, 127.92, 114.19, 55.93, 42.98, 22.85. HRMS ESI (+): Calculated for $C_{14}H_{24}O_3N_3S$ $[M+H]^+$: 314.15329; measured: 314.15274.

## 7. Fourier-Transform Infrared Attenuated Total Reflectance (FTIR-ATR) Spectra for Isolated Products 1-10

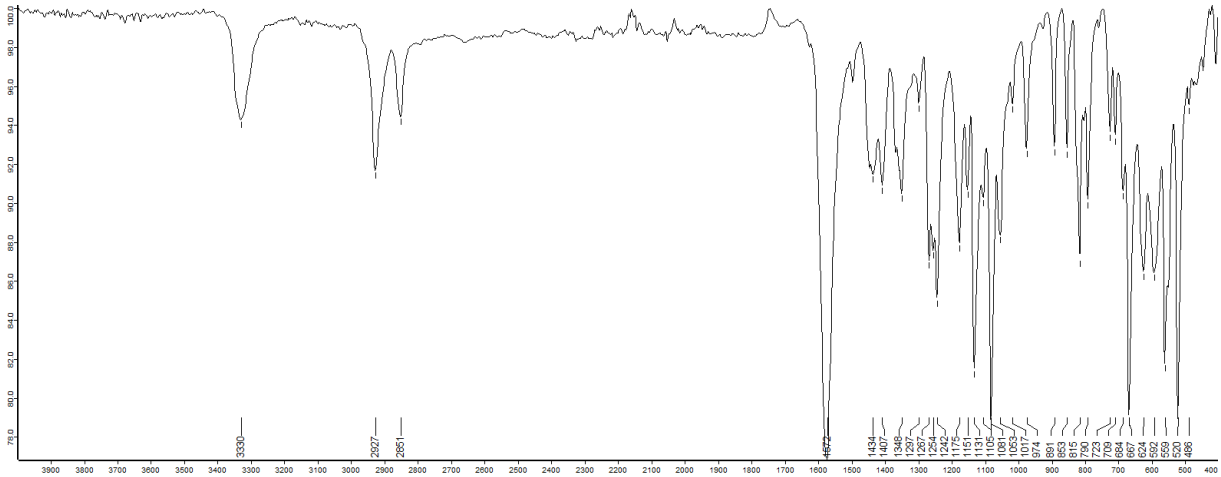


**Figure S3.** FTIR-ATR spectrum of isolated compound **1** Form I, synthesized by LA-RAM.

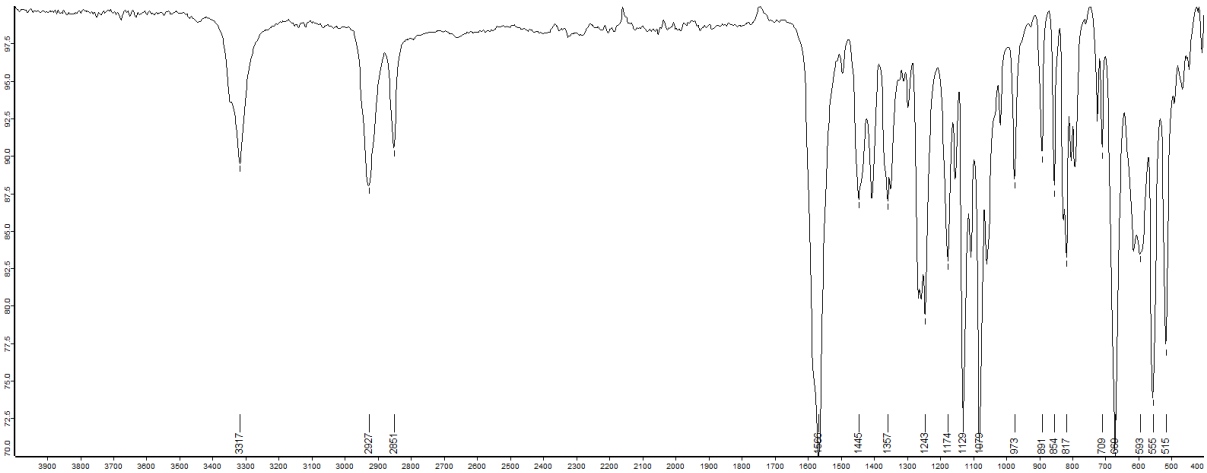


**Figure S4.** FTIR-ATR spectrum of isolated compound **1** Form II, synthesized by LA-RAM.

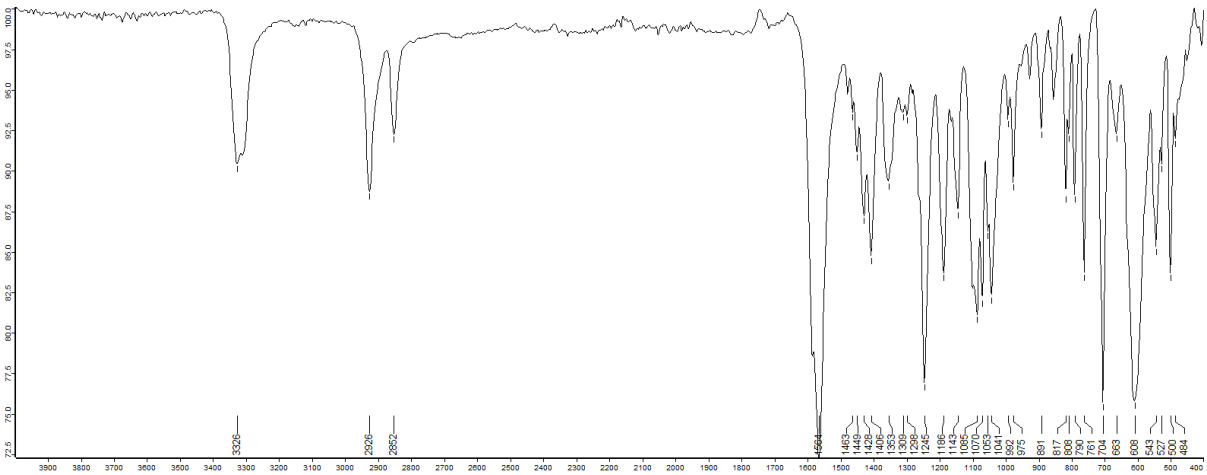


**Figure S5.** FTIR-ATR spectrum of isolated compound **2**, synthesized by LA-RAM.

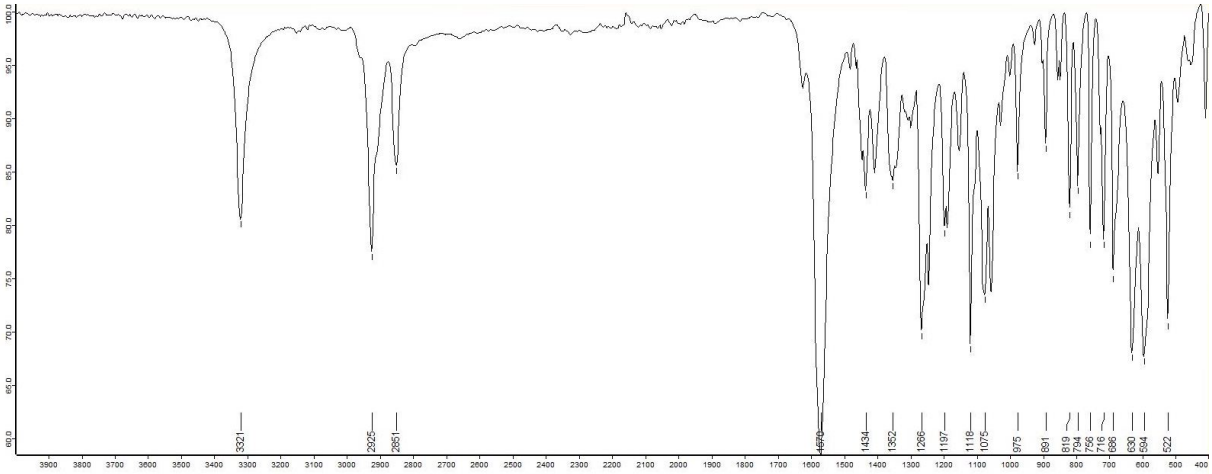


**Figure S6.** FTIR-ATR spectrum of isolated compound **3**, synthesized by LA-RAM.

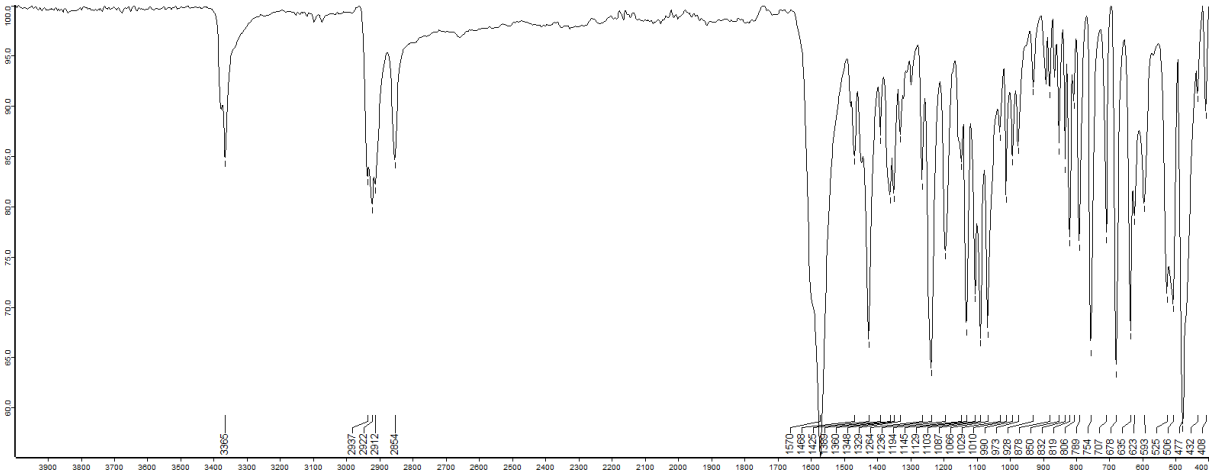


**Figure S7.** FTIR-ATR spectrum of isolated compound **4**, synthesized by LA-RAM.

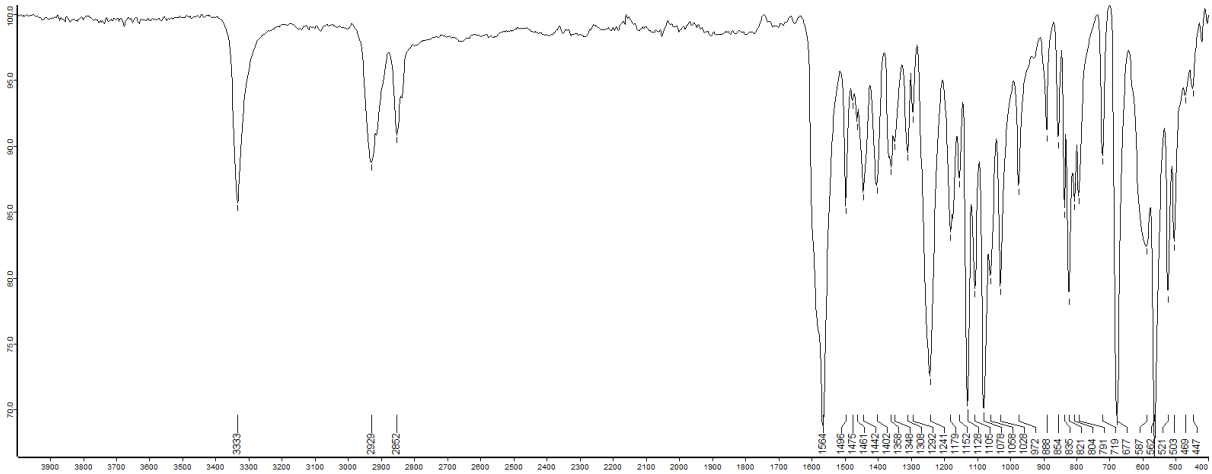


**Figure S8.** FTIR-ATR spectrum of isolated compound **5**, synthesized by LA-RAM.

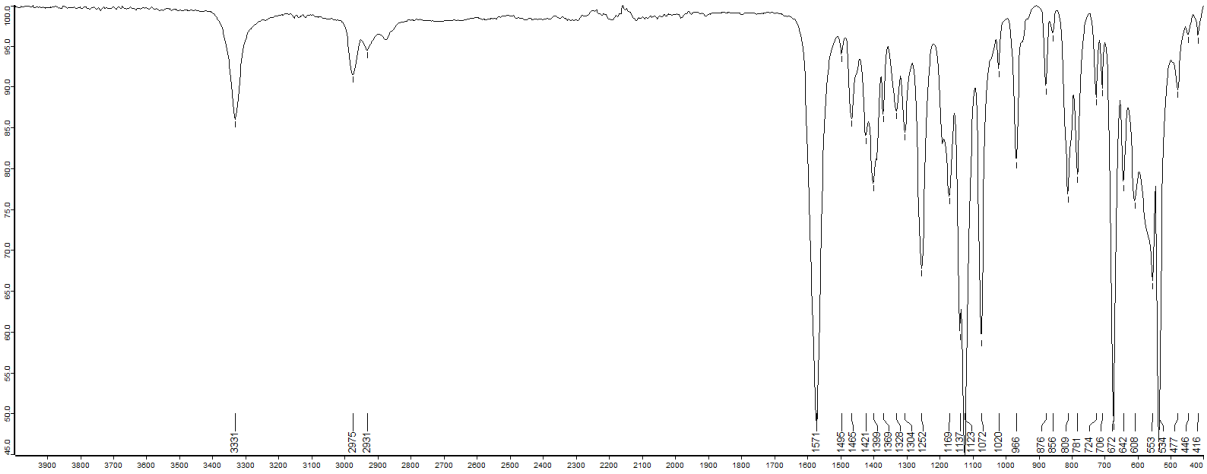

**Figure S9.** FTIR-ATR spectrum of isolated compound **6**, synthesized by LA-RAM.

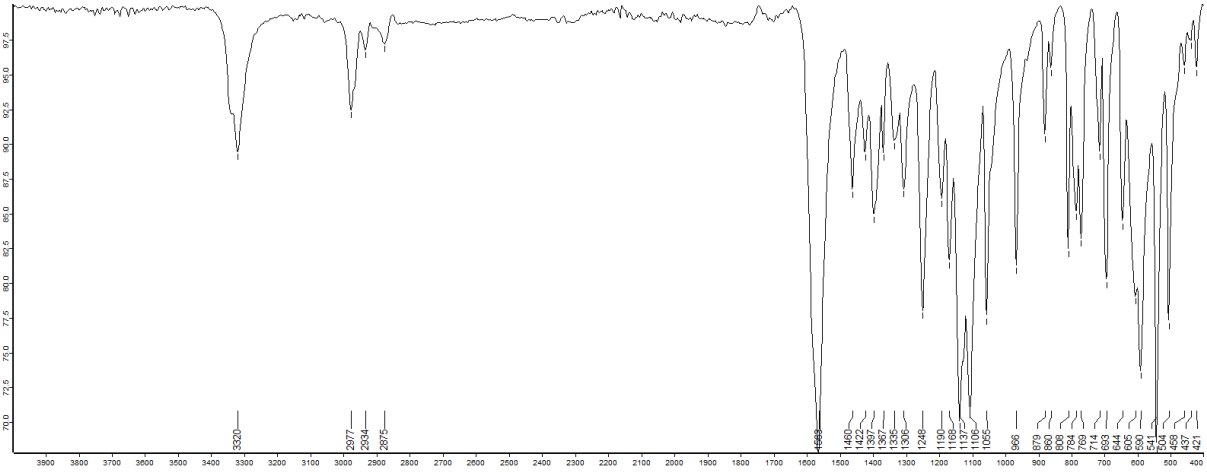

**Figure S10.** FTIR-ATR spectrum of isolated compound **7**, synthesized by LA-RAM.

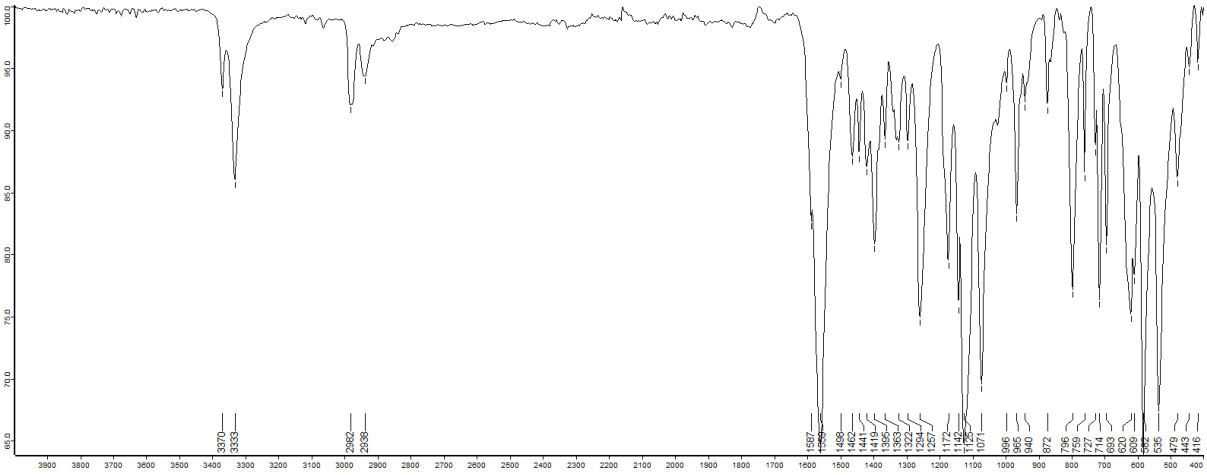

**Figure S11.** FTIR-ATR spectrum of isolated compound **8**, synthesized by LA-RAM.

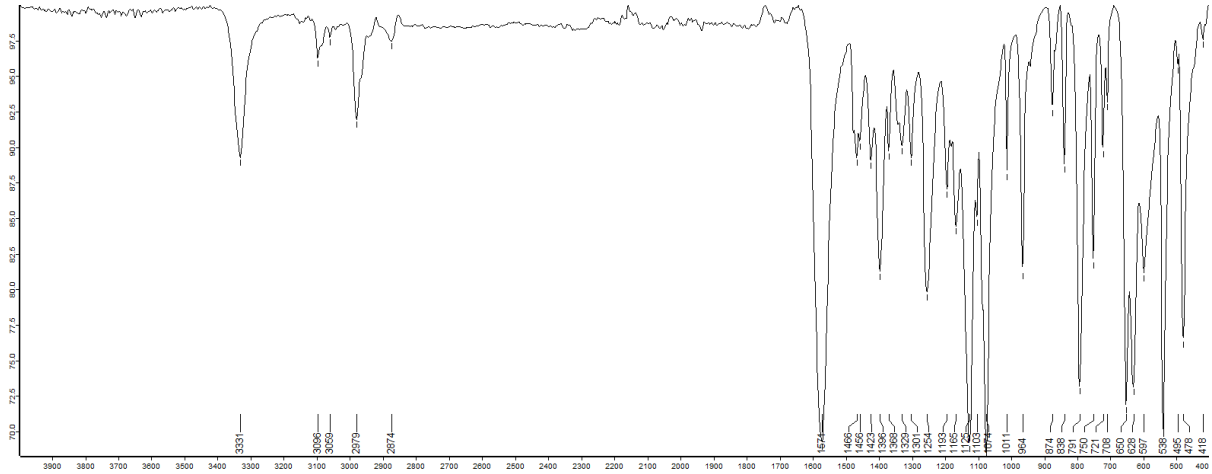


**Figure S12.** FTIR-ATR spectrum of isolated compound **9**, synthesized by LA-RAM.

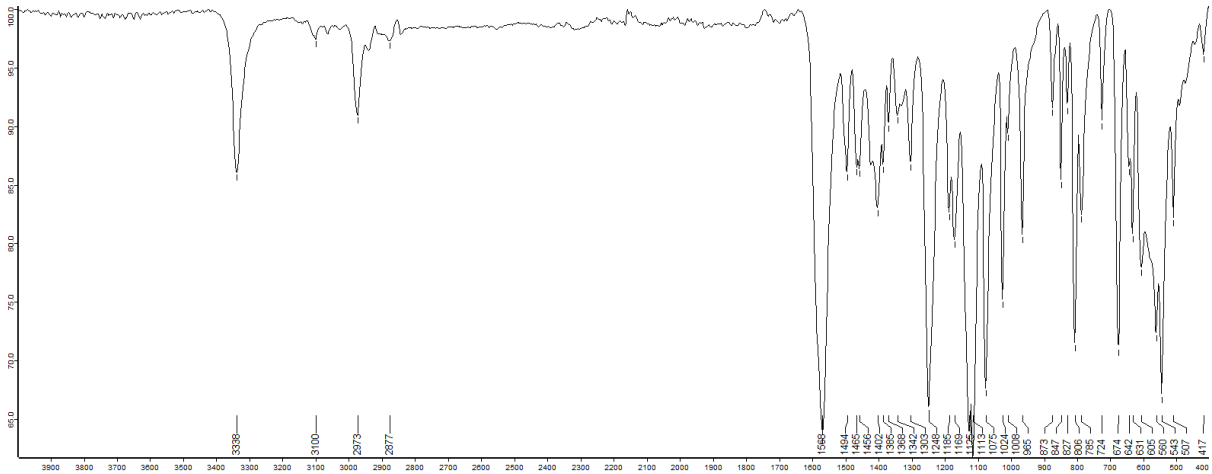


**Figure S13.** FTIR-ATR spectrum of isolated compound **10**, synthesized by LA-RAM.

## 8. $^{1}H$ and $^{13}C$ NMR Data for Isolated Products 1-10

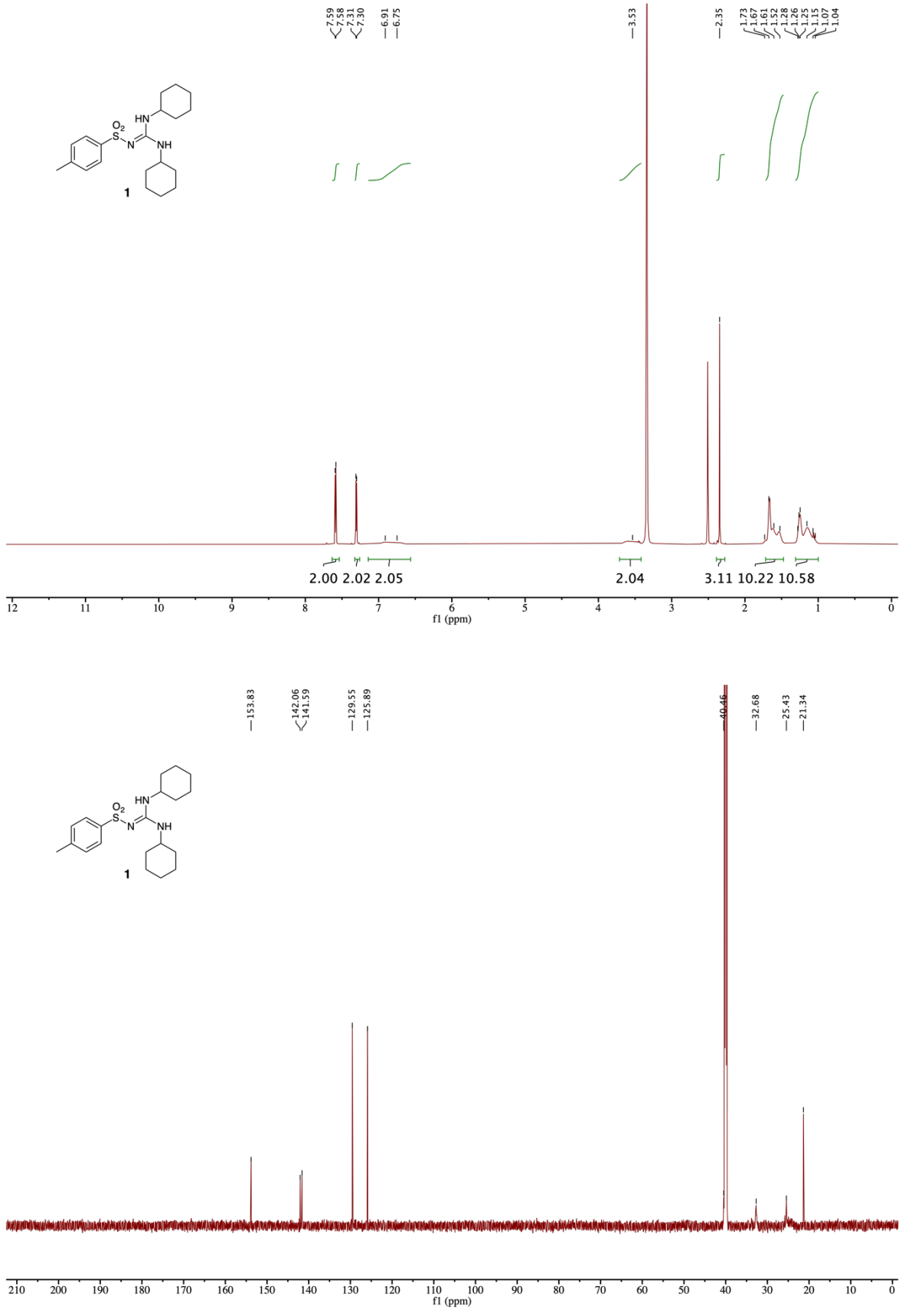


**Figure S14.** (top) $^{1}H$ and (bottom) $^{13}C$ NMR spectra for isolated compound **1**, synthesized by LA-RAM.

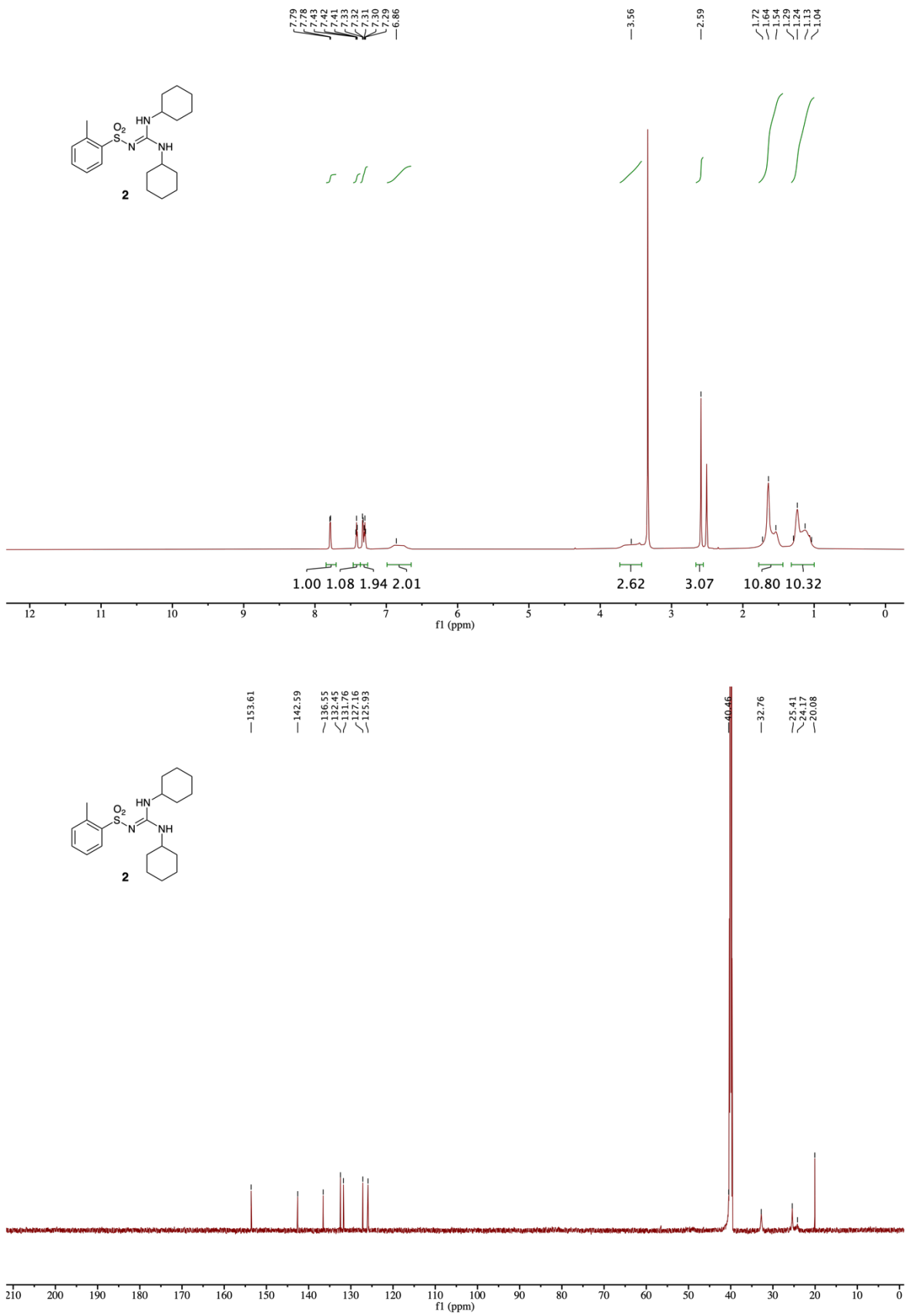


**Figure S15.** (top) $^{1}H$ and (bottom) $^{13}C$ NMR spectra for isolated compound **2**, synthesized by LA-RAM.

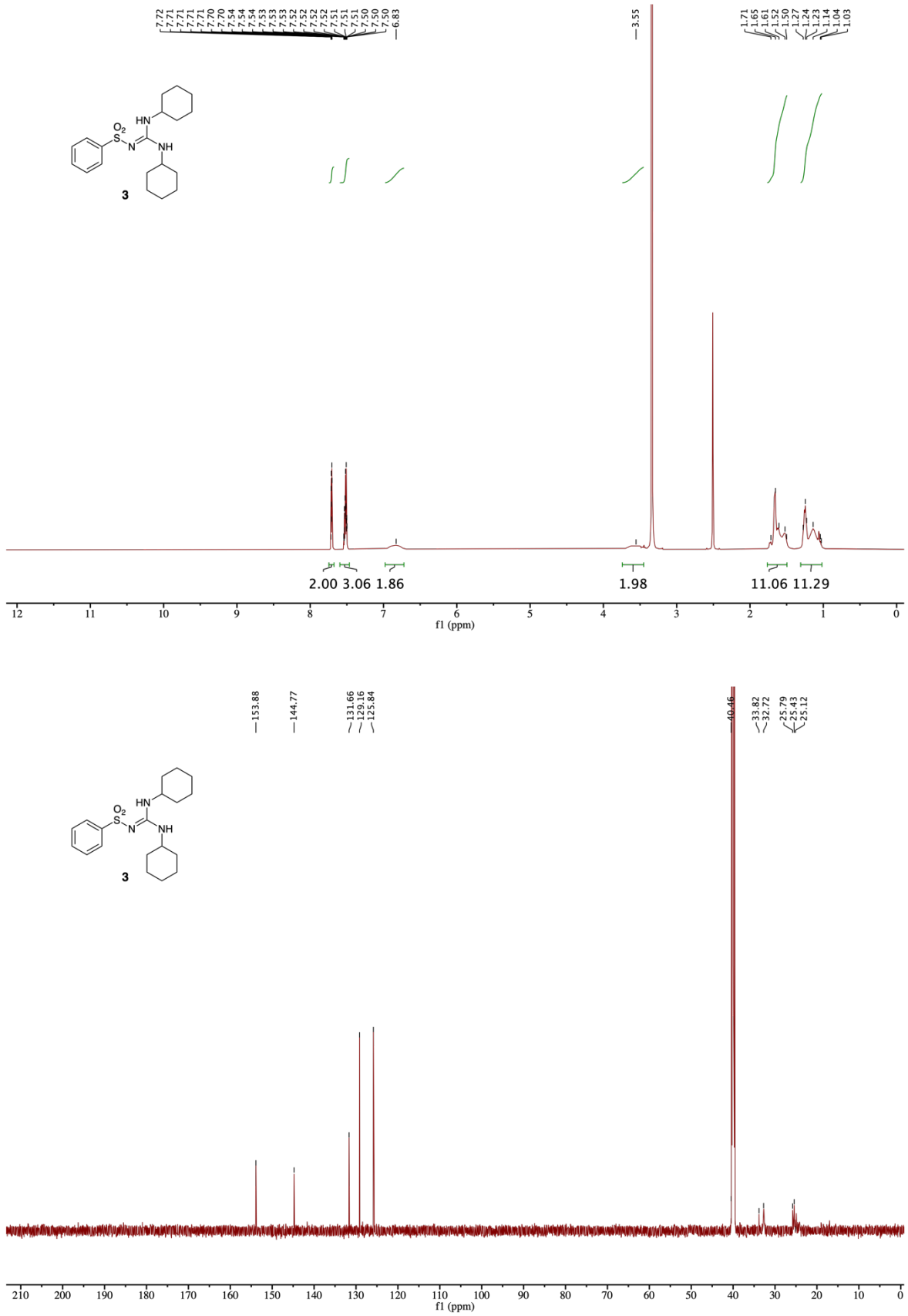


**Figure S16.** (top) $^{1}H$ and (bottom) $^{13}C$ NMR spectra for isolated compound **3**, synthesized by LA-RAM.

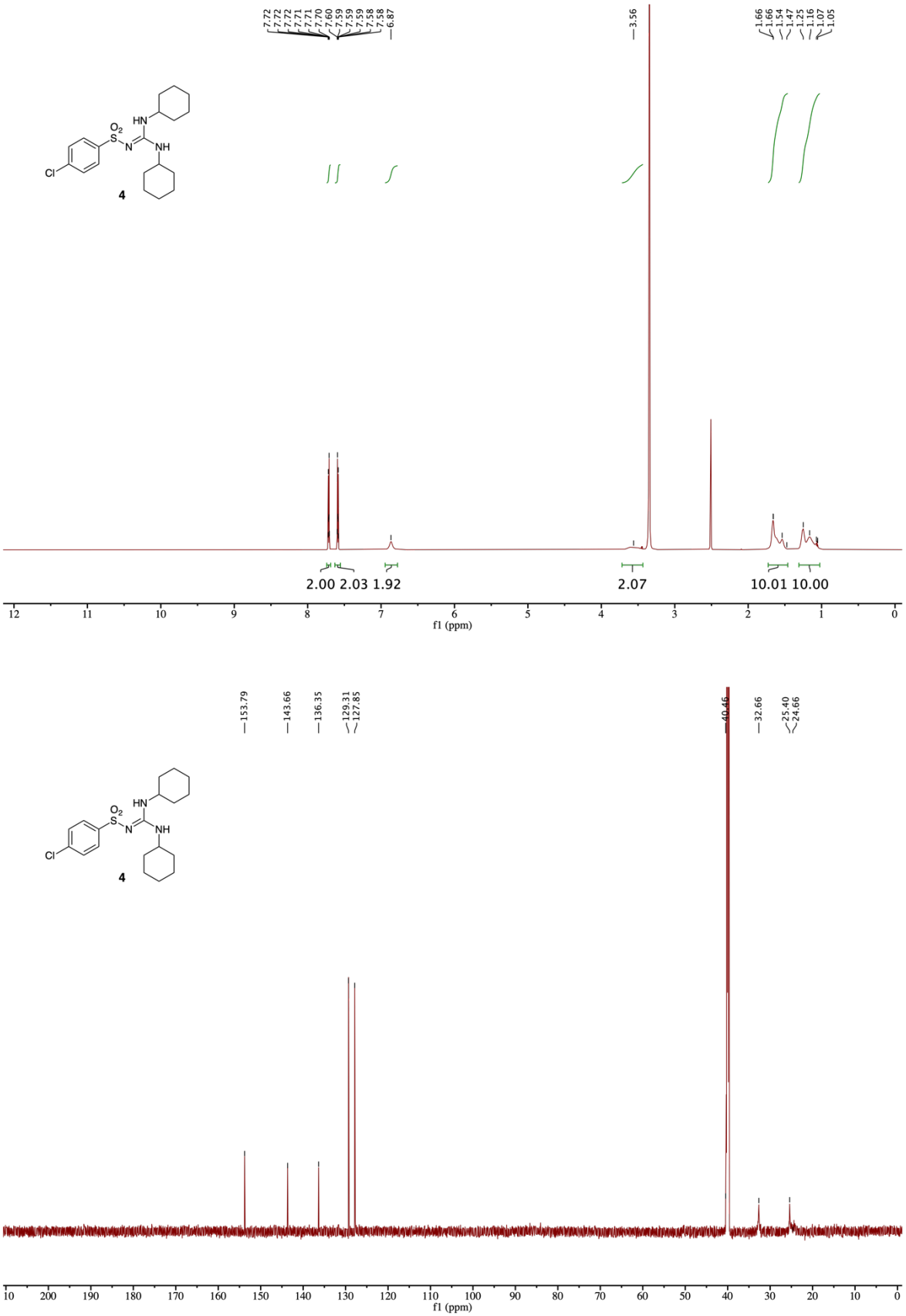


**Figure S17.** (top) $^{1}$H and (bottom) $^{13}$C NMR spectra for isolated compound **4**, synthesized by LA-RAM.

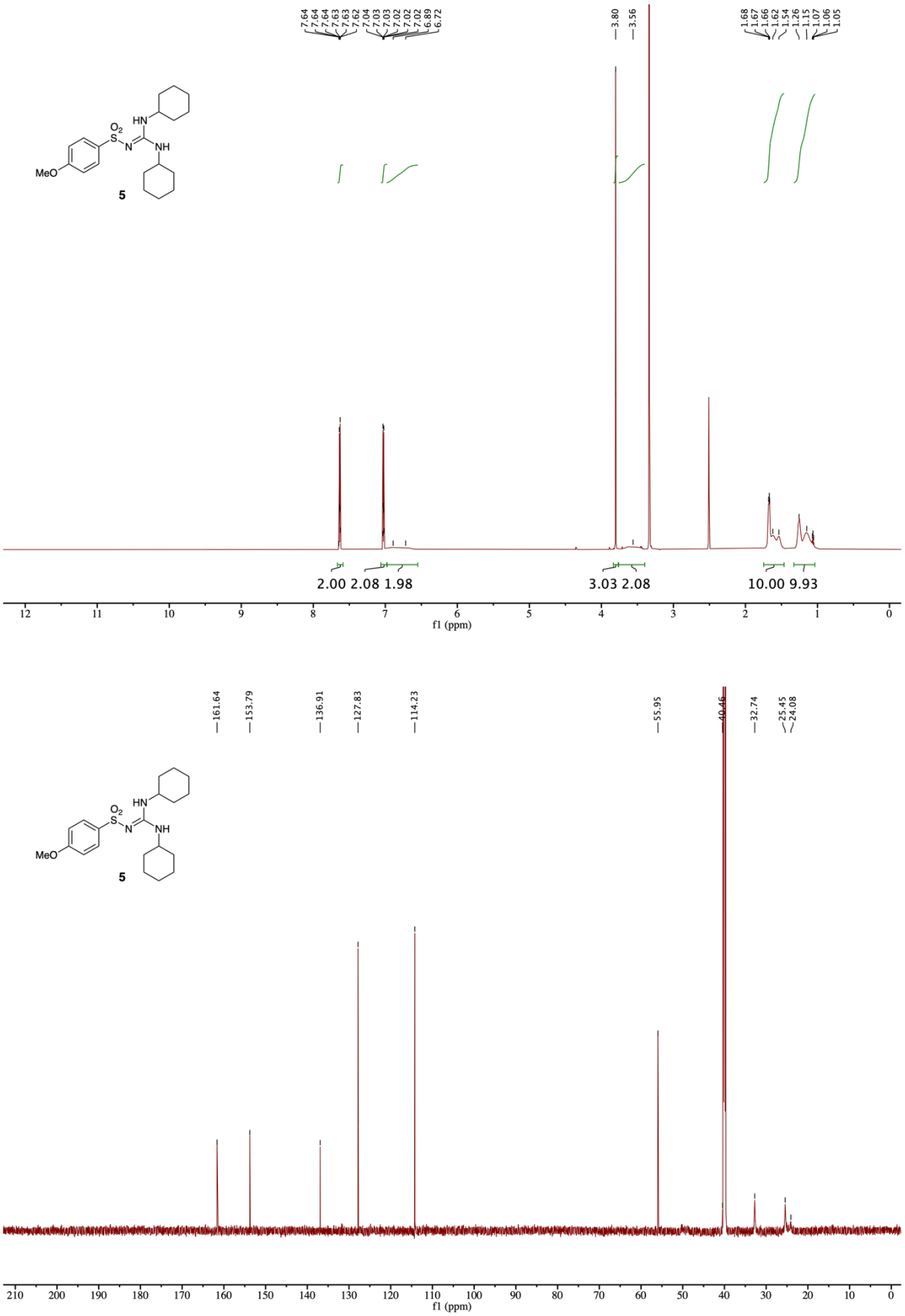


**Figure S18.** (top) $^{1}H$ and (bottom) $^{13}C$ NMR spectra for isolated compound **5**, synthesized by LA-RAM.

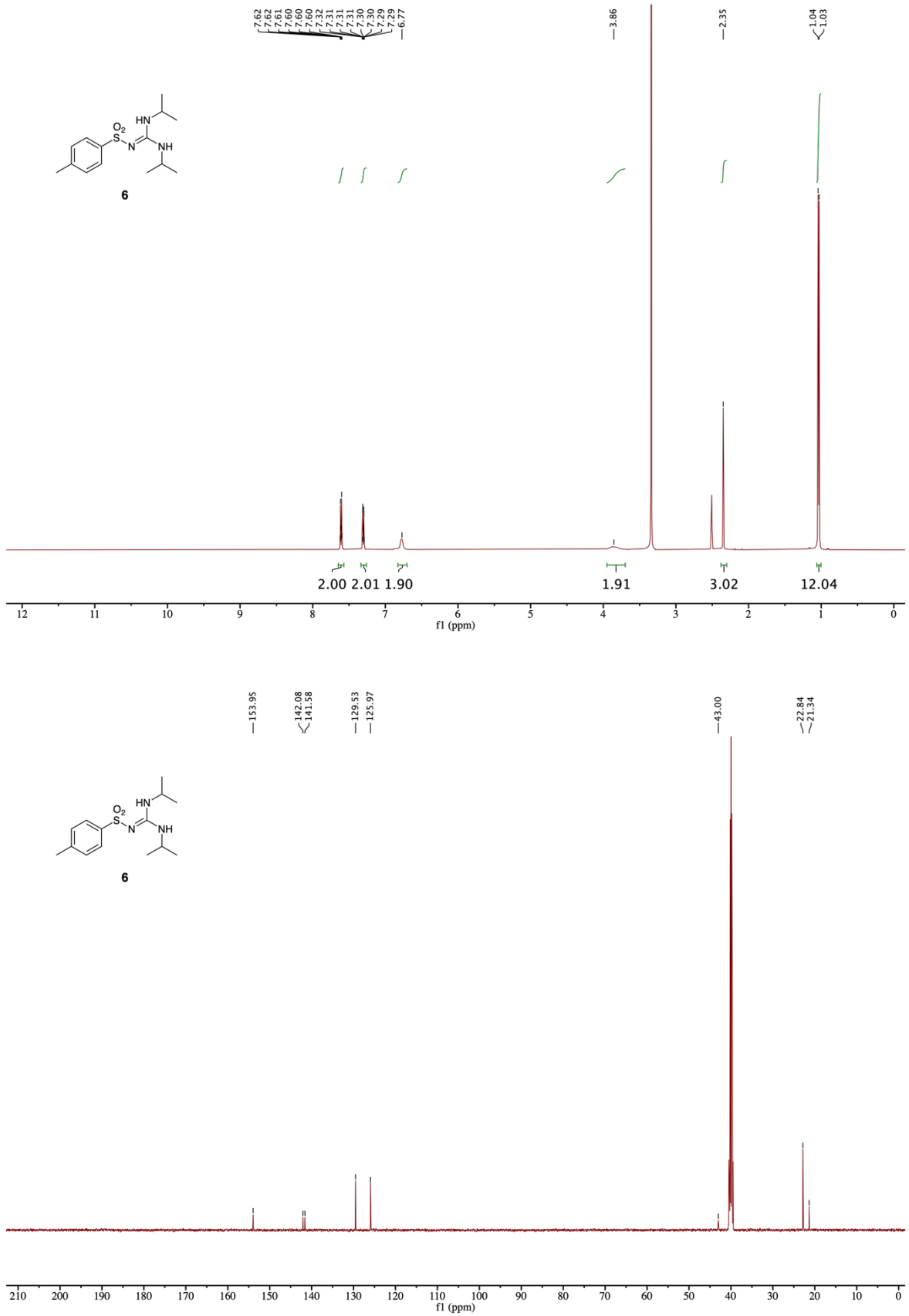


**Figure S19.** (top) $^{1}H$ and (bottom) $^{13}C$ NMR spectra for isolated compound **6**, synthesized by LA-RAM.

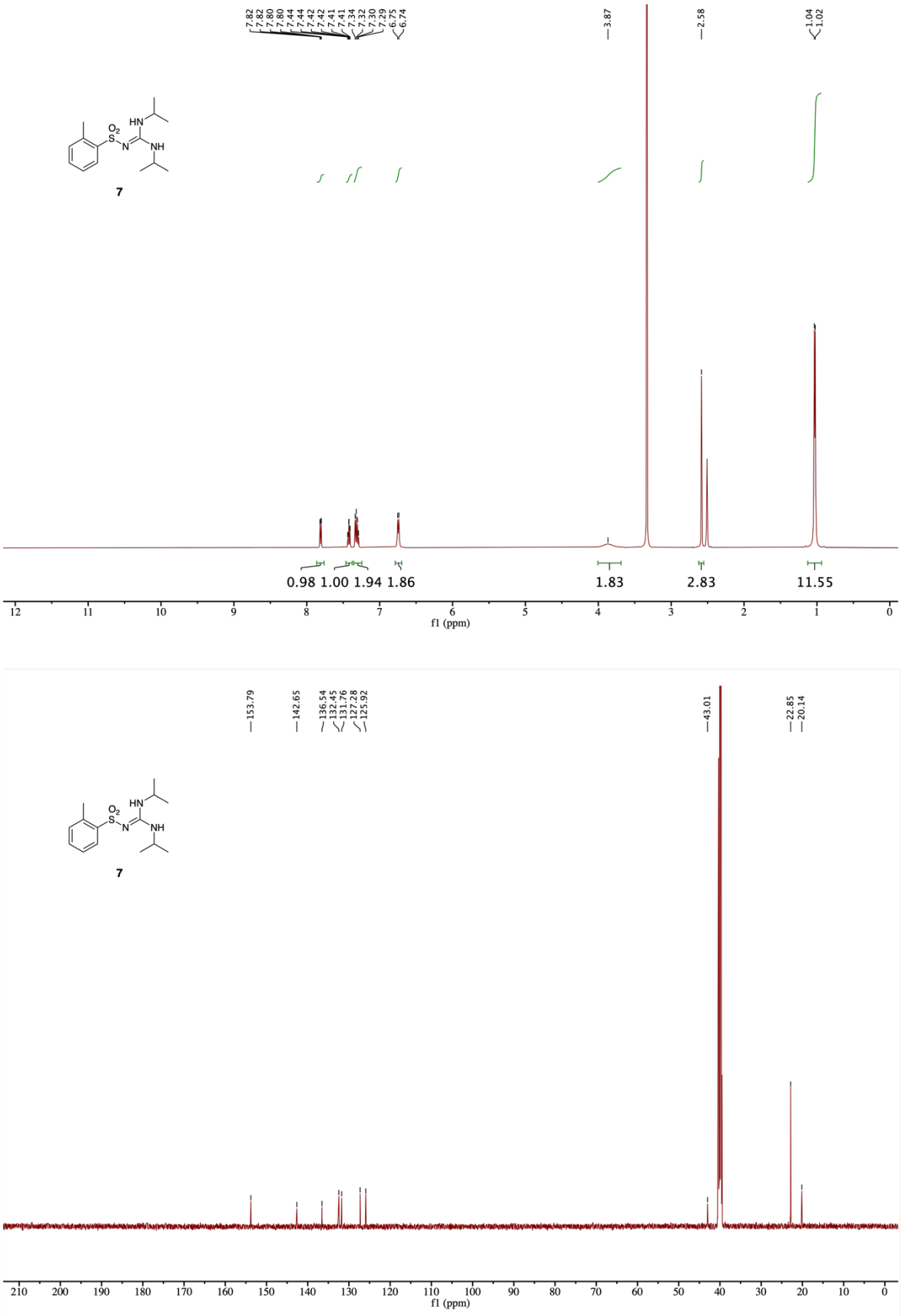


**Figure S20.** (top) $^{1}H$ and (bottom) $^{13}C$ NMR spectra for isolated compound **7**, synthesized by LA-RAM.

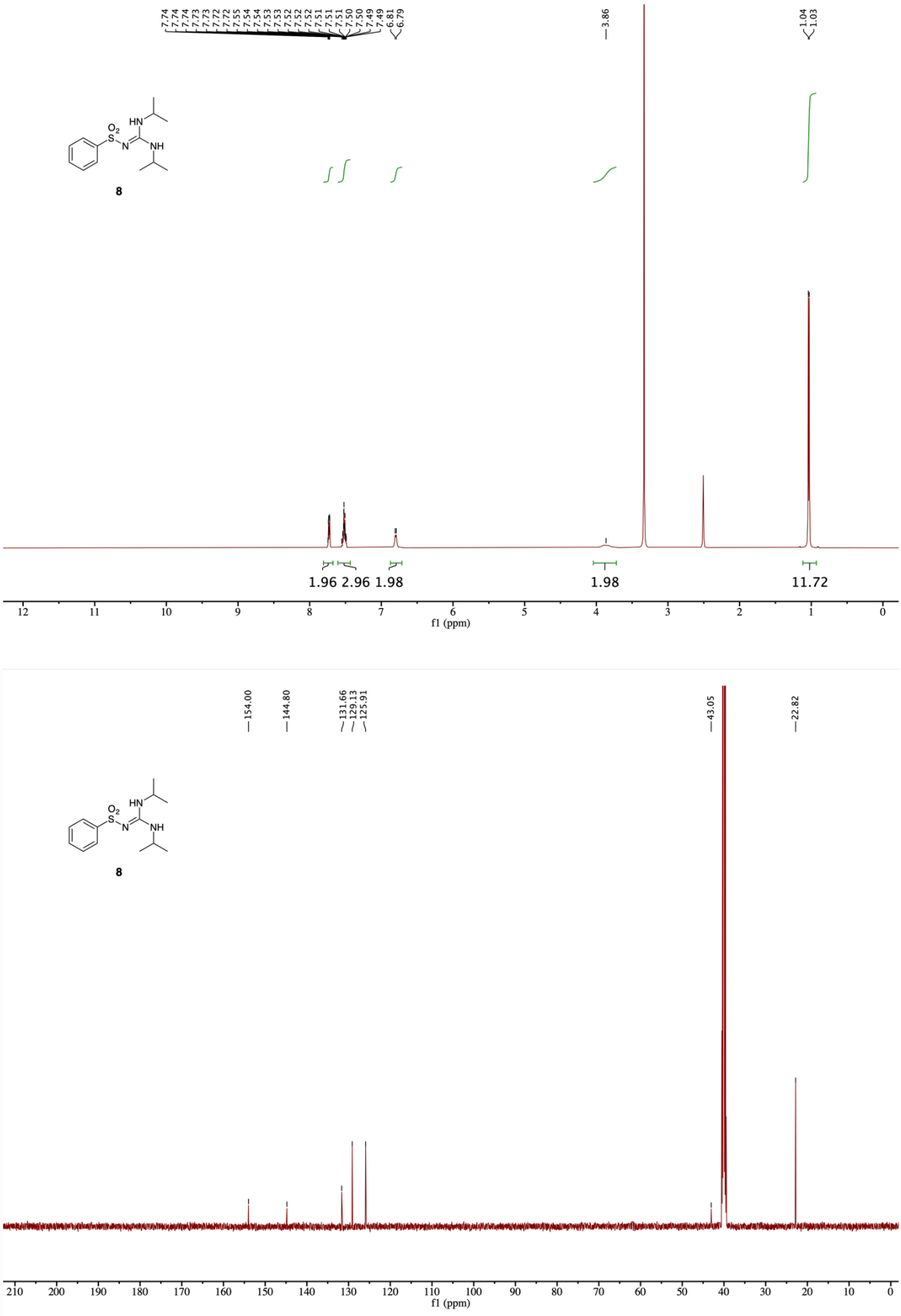


**Figure S21.** (top) $^{1}H$ and (bottom) $^{13}C$ NMR spectra for isolated compound **8**, synthesized by LA-RAM.

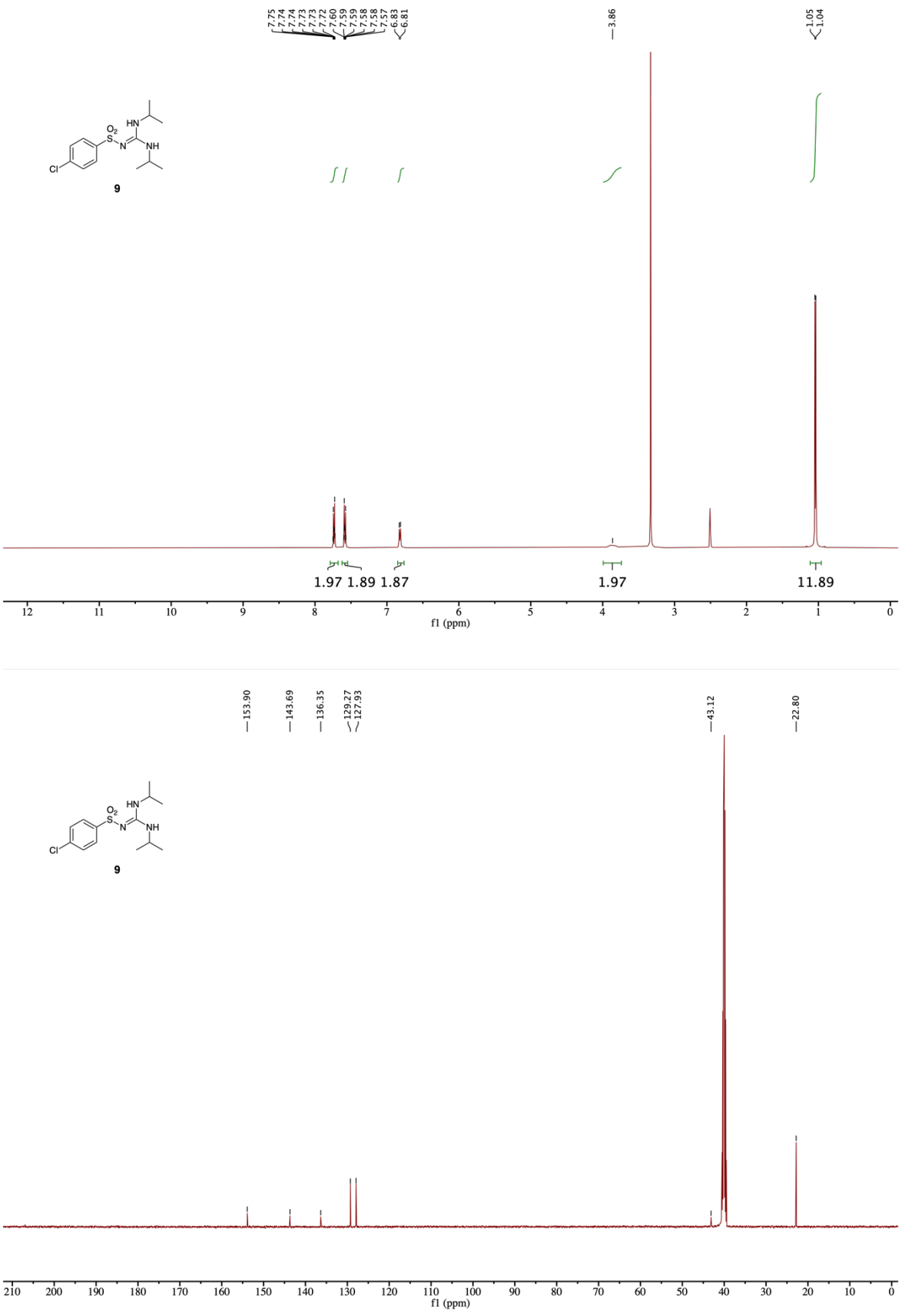


**Figure S22.** (top) $^{1}H$ and (bottom) $^{13}C$ NMR spectra for isolated compound **9**, synthesized by LA-RAM.

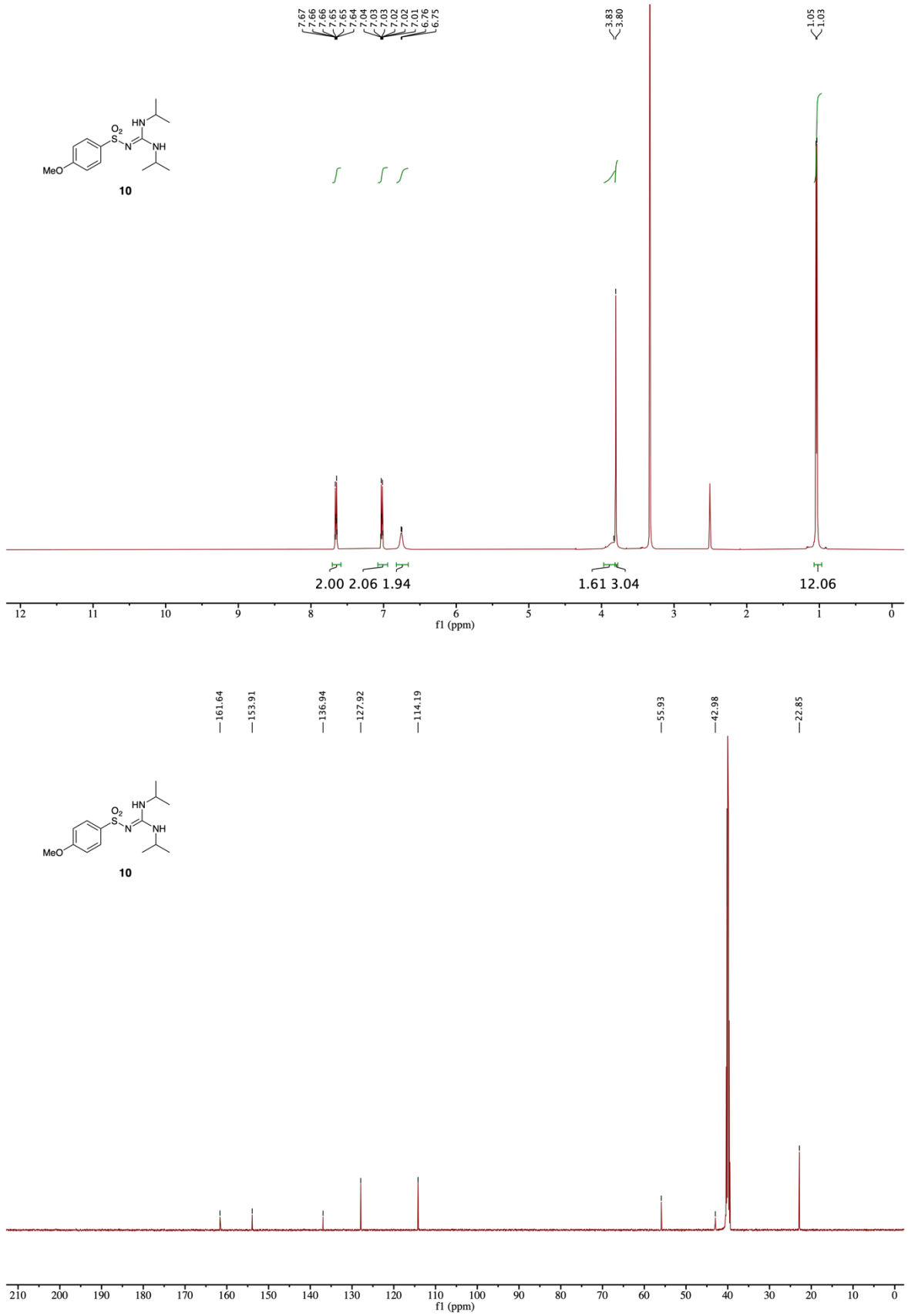


**Figure S23.** (top) $^{1}H$ and (bottom) $^{13}C$ NMR spectra for isolated compound **10**, synthesized by LA-RAM.

## 9. Theoretical modelling

The plane-wave basis set was truncated at 650 eV cutoff and the 1st electronic Brillouin zone was sampled with $2\pi \times 0.07$ Å$^{-1}$ Monkhorst-Pack grid k-point spacing.[5] Tight convergence criteria were used in the optimisation, namely: $5\text{x}10^{-6}$ eV atom$^{-1}$ for total energy; 0.01 eV Å$^{-1}$ for atomic forces; $5 \times 10^{-4}$ Å for atomic displacement and 0.02 GPa for residual stress.

The validity of the three approaches (PBE+TS, PBE+D3 and PBE+D3+BJ) was evaluated by exploring the variation between measured and calculated crystallographic unit cell parameters (unit cell edges and volume, *V*) for each method (Table S5, Figures S24, S25). Comparing the variation between calculated crystallographic parameters and the measured parameters indicate that both PBE+D3 and PBE+D3+BJ provide accurate structural models of Form I and Form II, whereas PBE+TS deviates substantially from the observed values.

**Table S5.** Overview of the crystallographic unit cell parameters that were experimentally determined for Form I and II of compound **1**, to the corresponding values after optimisation using periodic DFT methods PBE-TS, PBE-D3 and PBE-D3-BJ.

| Form I | | | | | | | | |
|---|---|---|---|---|---|---|---|---|
| method | *a* (Å) | *b* (Å) | *c* (Å) | *α* (º) | *β* (º) | *γ* (º) | *V* (Å$^3$) | % change of V |
| experiment | 12.075(3) | 12.703(3) | 15.167(4) | 92.220(3) | 109.140(3) | 106.008(3) | 2091.14 | 0 |
| PBE+TS | 11.9028 | 12.5658 | 14.7976 | 92.3639 | 108.2007 | 105.9205 | 2002.26 | -4.2503 |
| PBE+D3 | 12.0033 | 12.6045 | 15.1228 | 92.3827 | 109.056 | 106.101 | 2055.69 | -1.6952 |
| PBE+D3-BJ | 11.9912 | 12.605 | 14.989 | 92.344 | 108.624 | 105.993 | 2043.11 | -2.2968 |
| Form II | | | | | | | | |
| experiment | 23.2800(4) | 23.2800(4) | 19.9119(4) | 90 | 90 | 120 | 9345.65 | 0 |
| PBE+TS | 22.9287 | 22.987 | 19.5264 | 90 | 90 | 120 | 8890.23 | -4.8731 |
| PBE+D3 | 23.1187 | 23.1187 | 19.7085 | 90 | 90 | 120 | 9112.44 | -2.4954 |
| PBE+D3-BJ | 23.0809 | 23.0809 | 19.6763 | 90 | 90 | 120 | 9077.78 | -2.8663 |

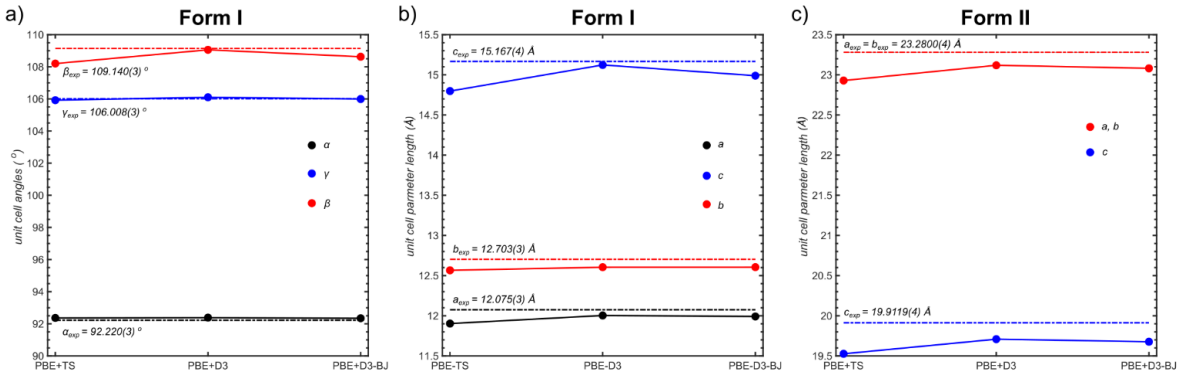


**Figure S24.** Graphical comparison of the crystallographic unit cell parameters measured for Form I and Form II of compound **1** (dashed line) to the corresponding parameters optimised using periodic DFT approaches PBE-TS, PBE-D3 and PBE-D3-BJ (full circles and line): a) the unit cell angles *α*, *β*, and *γ* for Form I; b) the unit cell edges *a*, *b* and *c* for Form I; c) unit cell edges *a* and *c* for Form II. The experimentally determined values are designated $\alpha_{exp}$, $\beta_{exp}$, $\gamma_{exp}$, $a_{exp}$, $b_{exp}$ and $c_{exp}$.

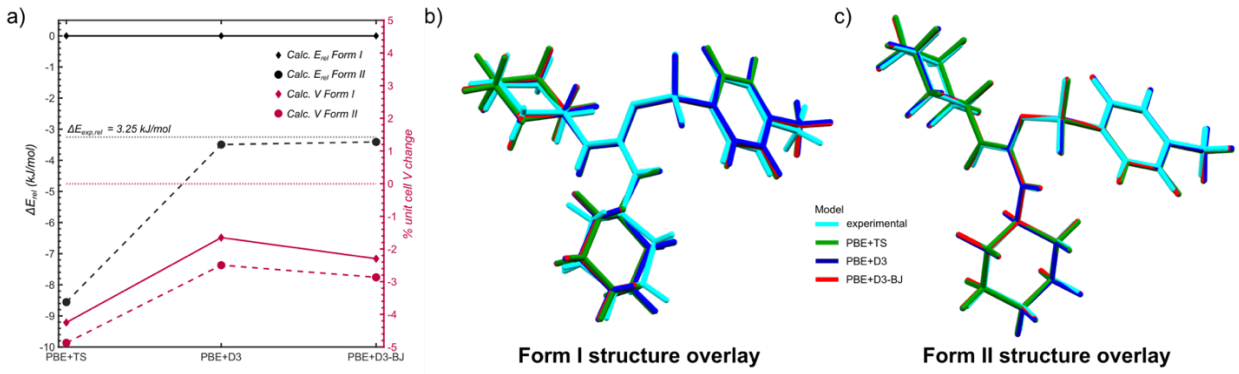


**Figure S25.** a) Comparison of the % difference of calculated crystallographic unit cell volumes ($V$) of Form I (red diamonds) and II (red circles) from the experimentally measured values, and a comparison of the calculated % difference in crystal energy between Form I and II ($E_{rel}$) to the value estimated from DSC data ($\Delta E_{exp,\ rel}$). As a guide, a value of 0% difference from experimentally determined unit cell volume, and the value of experimentally determined $\Delta E_{exp,\ rel}$ are shown as dotted horizontal black and red lines, respectively. Comparison of the experimentally observed molecular conformation for **1** to the conformations obtained from the optimised crystal structures using PBE+TS, PBE+D3 and PBE+D3+BJ methods for: b) Form I and c) Form II.

## References


1 G. M. Sheldrick. *Acta Cryst.,* 2015, **C71,** 3-8.
2 O. V. Dolomanoc, L. J. Bourhis, R. J. Gildea, J. A. K. Howard, and H. Puschmann, *J. Appl. Crystallogr.,* 2009, **42**, 339-341.
3 a) G. M. Sheldrick, *Acta Cryst.,* 2015, **A71**, 3-8. b) M. Sheldrick, SHELXTL Structure Determination Suite v.6.10, Bruker AXS, Inc., Madison, Wisconsin, USA, 2010.
4 C. B. Hübschle, G. M, Sheldrick, and B. Dittrich, *J. App. Cryst.*, 2011, **44**, 1281-1284.
5 H. J. Monkhorst and J. D. Pack, *Phys. Rev. B.,* 1976, **13**, 5188.


\